

Analysis and modeling of *Nannochloropsis* growth in lab, greenhouse, and raceway experiments

Patricia E. Gharagozloo · Jessica L. Drewry ·
Aaron M. Collins · Thomas A. Dempster ·
Christopher Y. Choi · Scott C. James

Received: 9 September 2013 / Revised and accepted: 24 January 2014 / Published online: 15 February 2014
© Springer Science+Business Media Dordrecht 2014

Abstract Efficient production of algal biofuels could reduce dependence on foreign oil by providing a domestic renewable energy source. Moreover, algae-based biofuels are attractive for their large oil yield potential despite decreased land use and natural resource (e.g., water and nutrients) requirements compared to terrestrial energy crops. Important factors controlling algal lipid productivity include temperature, nutrient availability, salinity, pH, and the light-to-biomass conversion rate. Computational approaches allow for inexpensive predictions of algae growth kinetics for various bioreactor sizes and geometries without the need for multiple, expensive measurement systems. Parametric studies of algal species include serial experiments that use off-line monitoring of growth and lipid levels. Such approaches are time consuming and usually incomplete, and studies on the effect of the interaction between various parameters on algal growth are currently lacking. However, these are the necessary precursors for computational models, which currently lack the data necessary to accurately simulate and predict algae growth. In this work, we conduct a lab-scale parametric study of the marine alga *Nannochloropsis salina* and apply the findings to our

physics-based computational algae growth model. We then compare results from the model with experiments conducted in a greenhouse tank and an outdoor, open-channel raceway pond. Results show that the computational model effectively predicts algae growth in systems across varying scale and identifies the causes for reductions in algal productivities. Applying the model facilitates optimization of pond designs and improvements in strain selection.

Keywords *Nannochloropsis* · Algae growth model · Computational fluid dynamics · Greenhouse · Open-channel raceway · Temperature · Light · CO₂ · Limitation · Salinity

Introduction

The high oil yield potential of algal biofuels (Chisti 2007; Mata et al. 2010) supports their development into commercialization as a renewable, carbon-neutral energy source (Singh and Gu 2010). Recent, techno-economic analyses show that algal biofuel is currently too expensive (US\$ 3.06 L⁻¹ TAG) to replace transportation fuels, but improvements in algae productivity and lipid yield could greatly reduce the cost (Sun et al. 2011). For a competitive algal biofuel, algae cultivation must be optimized.

Many factors contribute to the productivity of algae cultivation. Algal photoautotrophic growth is dependent on light intensity, temperature, salinity, pH, and availability of nutrients (US-DOE 2009; James and Boriah 2010; James et al. 2013). At low irradiance levels, light is limiting and insufficient energy (for photosynthesis) hinders growth rates. Conversely, irradiance above the optimal level may lead to oxidative stress (Li et al. 2009). Further, essential nutrients (carbon dioxide (CO₂), phosphate, sulfate, and nitrate) are critical to ensure that resources are available for growth and lipid production.

P. E. Gharagozloo (✉)
Sandia National Laboratories, PO Box 969, MS 9957, Livermore,
CA 94550, USA
e-mail: peghara@sandia.gov

J. L. Drewry · C. Y. Choi
University of Wisconsin, 460 Henry Mall, Madison, WI 53706, USA

A. M. Collins
Los Alamos National Laboratory, Los Alamos, NM 87545, USA

T. A. Dempster
Arizona State University, 7418 E. Innovation Way South, ISTB-3
203G, Mesa, AZ 85212, USA

S. C. James
Exponent, Inc, 320 Goddard Way, Suite 200, Irvine, CA 92618, USA

The temperature and pH ranges for optimal growth can be highly species/strain dependent and can vary from the low temperatures of the arctic to the high temperatures of the equatorial deserts (Lewis and Lewis 2005; Mayo 1997; Remias et al. 2005). When temperatures deviate from ideal, growth rates diminish (Eppley 1972). Salinity variations from optimal also decrease growth rates (Kirst 1989; Brock 1975; Auken and McNulty 1973; García et al. 2007; Fabregas et al. 1984; Batterton and Baalen 1971).

Large-scale bioreactor systems needed for commercial-scale biofuel production, open raceway ponds, and closed-photobioreactor systems often experience large spatiotemporal variations in environmental conditions over the course of a day, month, and year. Light conditions vary due to diurnal and annual cycles, fluctuations in cloud cover, the angle of the sun in the sky, and algae self-shading. The temperature of the bioreactor media depends on the reactor design, solar radiation, wind speed, air temperature, and evaporation. Nutrients vary due to varied consumption and delivery rates while pH depends on both extracellular (CO_2 concentration) and intracellular (species-dependent H^+) regulatory mechanisms (Katz et al. 1991). Salinity can vary due to evaporation and rainfall. These complex variations make it difficult to identify which parameters most affect the productivity of the culture.

A computational model that can predict the variations in the parameters affecting growth could aid in identifying which are most limiting for algae growth. Quinn et al. (2011) developed an algae growth and lipid production model of *Nannochloropsis oculata* for a specific design of an outdoor photobioreactor. Their model accounts for growth limitation due to light, temperature, and nitrogen. However, their model has only been validated for a single system and has not yet been applied to other bioreactor designs. Huesemann et al. (2013) developed a screening model specifically for raceway ponds. Their model accounts for light and temperature limitation but does not account for the variations in temperature within the pond nor does it predict the temperature based on meteorological data. James and Boriah (2010) developed a proof-of-concept model for algae growth in an open-channel raceway. Subsequently, James et al. (2013) verified the model against an analytical solution and then compared to experimental data. A simulation that is able to model multiple types of bioreactor systems and predict the cultivation pond conditions for locations around the globe is needed to properly optimize and design cultivation systems. Liffman et al. (2013) proposed new raceway pond geometries that reduced energy losses at the bends by 87 %.

In this work, we investigated the halophilic microalga, *Nannochloropsis*, that is a promising biofuel candidate (Pal et al. 2011; Boussiba et al. 1987). As with most algae strains, no complete parametric data have been published. Therefore, we must produce the data necessary to appropriately

parameterize our model for the algae strain of interest. To accomplish this, we grew the algae strain at various environmental conditions in laboratory test tubes and measured growth during the exponential growth phase. With this method, we were able to vary multiple parameters (i.e., light and salinity) simultaneously to reduce the time to complete the parametric study. In addition, the small size ensured that environmental conditions were constant across the sample and reduced the amount of algae mass needed to be grown.

The numerical simulations in this work used a modified version of the US Army Corp of Engineers water quality code (CE-QUAL) (Cercio and Cole 1995; James and Boriah 2010; James et al. 2013) to simulate algal growth kinetics in well-mixed photobioreactor-type systems. The model allows the flexibility to manipulate a host of variables associated with algal growth such as temperature, pH, light intensity, and nutrient availability. Salinity of the medium is another important operational parameter governing algal growth; the effects of salinity were added to the model to expand its capabilities to marine algae. To populate the model's empirical parameters, we conducted a parametric growth rate measurement of *Nannochloropsis salina* at different temperatures, light intensities, and salinities. The effect of pH was not investigated in this study due to the desire to have consistent CO_2 levels for each of the conditions. The computational fluid dynamics code ANSYS FLUENT (Fluent 2012) was used to model the heat transfer and algae transport. The model was then validated by comparing predictions from the lab-scale parameterized model to experimental results from both a greenhouse pond and outdoor, open-channel raceway. We showed that our model has excellent agreement for multiple bioreactor systems and can effectively predict the pond temperature based on meteorological data.

Materials and methods

We cultivated two similar strains of *Nannochloropsis*: *Nannochloropsis salina* CCMP 1776 and *Nannochloropsis granulata* LRB-MP-0209. Both were grown in *f/2* medium (Guillard and Ryther 1962). We grew *N. salina* at Sandia National Laboratories in a $25 \times 115 \text{ mm}^2$ quartz test tube at the Livermore, California, USA site to parameterize the model and in greenhouse tanks at the Albuquerque, New Mexico site. *N. granulata* was grown in an outdoor raceway at the Arizona Center for Algae Technology and Innovation at Arizona State University in Mesa, Arizona.

Light absorptivity

Light utilization by algae depends on the optical properties of photosynthetic pigment within the cell. While the absorptivity of pigments is generally known in select organic solvents,

light extinction is undoubtedly different in vivo. Therefore, we developed a quantitative relationship between pigment optical depth from the fluid surface (as a function of wavelength) and dry cell weight for *N. salina*, thus, identifying the absorptivity at all wavelengths.

In brief, duplicate scatter-free absorbance measurements across six different sample concentrations of *N. salina* were obtained using a 60-mm integrating sphere attached to a PerkinElmer, Lambda 950 spectrophotometer. An integrating sphere was used to remove the contribution of scatter from the algal and detritus in the sample. In parallel, cell counts were used to determine the concentrations of these samples (concentrations ranged from 3.75×10^6 to 7.5×10^7 cells mL^{-1}). Classical least squares (CLS) was used to project these concentrations onto the spectral data to obtain the pure component spectral estimate that represents the absorptivity of *Nannochloropsis*. This calculation was conducted with MATLAB (2013) and consisted of multiplying the pseudo-inverse of the concentrations by the measured spectra to obtain this pure component estimate. Further details of this CLS method can be found elsewhere (Haaland et al. 1985).

Lab-scale model parameterization

N. salina was grown in *f/2* media in a laboratory incubator with a diurnal cycle of 16:8 (light/dark). We adapted the cultures to light conditions, NaCl concentrations, and temperatures. Algae were grown in 25-mm test tubes with air bubbled through a plastic tube submerged to the bottom of the test tube to provide CO_2 and mixing. The pH was monitored daily for each sample with a submersible, calibrated meter (Omega Engineering, Inc/PHB21) and was consistently between 7.5 and 8.0. This range is within the optimal pH range for *N. salina* between 7.5 and 9.0 (Bartley et al. 2013; Boussiba et al. 1987). Changes in cell concentration were estimated using a calibrated digital fluorometer (Turner Designs/10-AU) to measure the chlorophyll *a* fluorescence in vivo. The fluorometer transmits an excitation beam of light in the 440-nm range and detects light emitted from the sample in the 680-nm range. The measurements were calibrated to initial culture cell counts at each light intensity and the fluorescence was measured daily to produce growth curves for each offset of experimental conditions. To compare with the model, the fluorescence measurements are converted to cell counts based on the initial calibration and then converted to biomass concentration based on the measured cell mass of 2.7 pg cell^{-1} . Although chlorophyll fluorescence is not an appropriate method for measuring a quantitative biomass concentration, the change in fluorescence over time of a given sample during the exponential growth phase estimates the rate of change of the sample concentration or growth rate (Mayer et al. 1997; Seródio et al. 2001; Torzillo et al. 1996; Samuelsson and Öquist

2006; Sukenik et al. 2009; Masojidek et al. 2010; Vyhnalek et al. 1993). Growth rates were calculated from data measured in triplicate at three light conditions (10.5, 27, and 58 W m^{-2}), four NaCl concentrations (0.35, 0.5, 0.75, and 1 M), and four temperatures (18, 22, 26, $30 \text{ }^\circ\text{C}$). The concentration over time during the exponential growth phase is represented by the equation $C_{\text{chl}a}(t) = C_0 \exp(\mu t)$, where $C_{\text{chl}a}$ is the chlorophyll *a* concentration, C_0 is the initial chlorophyll *a* concentration, t is the time, and μ is the exponential growth rate. The growth rates are calculated by linear curve fits to data from the exponential growth phase to $\ln(C_{\text{chl}a}) = \mu t + \ln(C_0)$ and averaged over the triplicate samples for each growth condition.

Greenhouse tanks experiment

A 40-L culture of laboratory-grown *N. salina* in *f/2* media was used to inoculate two circular tanks continuously mixed by a jet system enclosed in a greenhouse located in Albuquerque, NM. Each vessel had a radius of 0.9 m and a medium depth of 0.211 m. The initial nitrate and phosphate concentrations were 54.7 and 3.1 g m^{-3} . The two tanks were operated at different CO_2 levels. The first tank was bubbled with CO_2 levels elevated at 85 L h^{-1} with the other tank at ambient CO_2 levels. Temperature and pH were monitored with a submersible, calibrated meter (YSI Inc.). The pH remained between 8.0 and 8.5 for the ambient tank and between 7.4 and 7.8 for the elevated CO_2 tank during the course of the measurements. The pH was only briefly below 7.5 during the first days of the elevated- CO_2 tank measurement. Again, these values are within the range for ideal growth. Irradiance was monitored with a calibrated spectroradiometer (Ocean Optics). Biomass was estimated by comparing the optical density at 750 nm of each cultivation condition to a standard curve of biomass versus optical density generated for *N. salina*.

Open-channel raceway experiment

A 12-m^3 open raceway pond with a 20-cm culture depth was inoculated with nutrients ten times the standard *f/2* media. A filtered ambient air/ CO_2 mixture (1.5–2.0 % CO_2) is bubbled intermittently into the raceway pond through an airstone sparger to provide CO_2 to the algae culture for the purpose of maintaining a fairly constant pH between 7.8 and 7.9. To determine the algae concentration, dry weight and ash-free dry weight values were measured daily (Laurens et al. 2012). The pond temperature was measured and recorded at 15-min intervals using a Yellow Springs Instruments YSI 5200A-DC Multiparameter Water Quality Monitoring Unit approximately 10 cm below the surface. Light intensity was measured with the same calibrated spectroradiometer described above.

Algae growth model

The governing equation for algal biomass growth in CEQUAL is (Cercio and Cole 1995):

$$\frac{\partial B}{\partial t} = (P - B_M - P_R)B + \frac{\partial}{\partial z}(w_s B) + \frac{B_L}{V} \quad (1)$$

where B is the biomass, t is time, P is the production (growth) rate, B_M is the basal metabolic rate, P_R is the predation rate, w_s is the settling velocity, B_L represent external loads such as deposition or sources, and V is the model cell volume. Biomass production rates are determined by the availability of nutrients (including CO_2), the intensity of light, local temperature, pH, and salinity. For this work, the effects of salinity are considered while the effects of pH are neglected. The effect of each is considered to be multiplicative and decoupled (Cercio and Cole 1995):

$$P = P_M f(\nu) g(I) h(T) i(S) j(\text{pH}) \quad (2)$$

Here, P_M is the maximum instantaneous growth rate under optimal conditions; $f(\nu)$ is the effect of non-optimal nutrients, which includes CO_2 limitation ($0 \leq f(\nu) \leq 1$); $g(I)$ is the effect of non-optimal illumination ($0 \leq g(I) \leq 1$); $h(T)$ is the effect of non-optimal temperature ($0 \leq h(T) \leq 1$); $i(S)$ is the effect of non-optimal salinity ($0 \leq i(S) \leq 1$); and $j(\text{pH})$ is the effect of non-optimal pH ($0 \leq j(\text{pH}) \leq 1$). All of these functions are spatially dependent, and their values vary from cell to cell in the model according to local nutrient concentrations (including CO_2), incident solar radiation, salinity, and temperature.

For the lab-scale parameterization of the algae growth model, algae were grown in well-mixed lab conditions and the effects of predation, settling, pH, and CO_2 limitation can be neglected. In addition, for the initial validation study, the larger scale systems are assumed to obey the same conditions defined at the lab scale. It is acknowledged that this may not hold true and future studies will address these components of the model. The basal metabolism rate varies with temperature according to:

$$B_M(T) = B_M(T_0) \exp[K_{T_B}(T - T_0)] \quad (3)$$

where T_0 is 20°C and $B_M(T_0)$ is set to 0.01 day^{-1} , and K_{T_B} is the effect of temperature on the metabolism and is set to 0.069°C^{-1} (Cercio and Cole 1994). This results in the basal metabolic rate increasing to 0.03 day^{-1} at 36°C . These are general values for algae due to a lack of published data available for specific strains. While this parameter is uncertain, the fitted growth rate will largely account for error in the basal metabolism rate, δB_M . The algae growth model is implemented in the commercial computational fluid

dynamics code ANSYS FLUENT (Fluent 2012) to allow for fluid flow and heat transfer calculations in a wide variety of systems.

Two types of domains are used for the current study. First is a simplified single-cell rectangular domain with dimensions representative of the experiment, which assumes the culture is well-mixed and conditions such as light intensity and temperature are uniform within the culture. However, the light intensity changes as the culture density increases (which the model accounts for), while the temperature remains constant. We determine at which scale and conditions it is no longer appropriate to use the simplified domain and expand the complexity of the domain to account for the spatial variations in the light and temperature conditions. The second domain is a 2D rectangular representation of the raceway pond. Both domains are shown in Fig. 1.

Model parameterization

Model parameterization occurs in two steps. First, limitation functions (described below) are fit individually to the normalized measured growth rate versus the growth variable (light intensity, temperature, and salinity) using CLS. Second, the maximum ideal productivity is fit to the growth data (described in the “Results and Discussion” section). To assess the agreement, the R^2 value is calculated according to:

$$R^2 = 1 - \frac{\sum (C_{\text{data}} - C_{\text{prediction}})^2}{\sum (C_{\text{data}} - \bar{C}_{\text{data}})^2} \quad (4)$$

where C_{data} is the concentration value of the data point, $C_{\text{prediction}}$ is the concentration predicted by the model at the same time, and \bar{C}_{data} is the average concentration for all the data points.

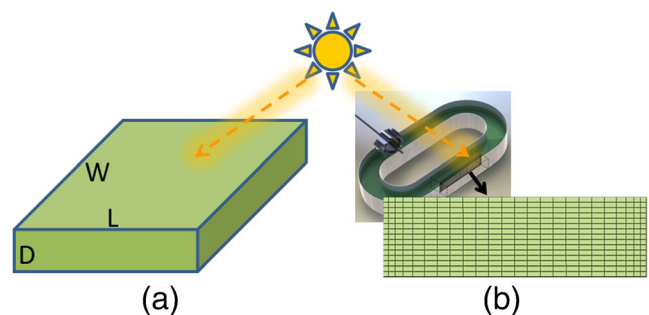


Fig. 1 Two solver domains used in study: (a) simplified single-cell rectangular domain and (b) meshed 2D rectangular representation of raceway pond

Nutrients

Growth limitation due to nutrient availability is based on the Monod equation (Monod 1949):

$$f(\nu) = \frac{\nu}{K_X^h + \nu} \tag{5}$$

where ν is the nutrient concentration and K_X^h is the half-saturation constant. For example, the nutrient function for green algae can be nutrient limited by dissolved ammonium, nitrate, phosphate, or CO₂, yielding:

$$f(\nu) = \min\left(\frac{NH_4 + NO_3}{K_N^h + NH_4 + NO_3}, \frac{PO_4}{K_P^h + PO_4}, \frac{CO_2}{K_C^h + CO_2}\right) \tag{6}$$

Here, NH₄ is the ammonium concentration, NO₃ is the nitrate concentration, PO₄ is the dissolved phosphate concentration, CO₂ is the dissolved carbon dioxide concentration, and K_N^h , K_P^h , and K_C^h are the corresponding half-saturation constants.

Half-saturation constants are typically defined for the low concentrations of nutrients common in environmental systems and are on the order of 0.01 g m⁻³. The half-saturation constants used in this model are 0.01 g m⁻³ (Cercu and Cole 1994), 0.002 g m⁻³ (Cercu and Cole 1994), and 0.028 g m⁻³ (Hecky et al. 1993) for nitrogen, phosphorous, and CO₂, respectively. For algal growth systems (raceways), nutrients are often added in excess and the nutrient limiting function is close to unity. However, CO₂ is often difficult to maintain at sufficient concentrations particularly during high-growth periods, in large reactors, and at high algae concentrations. Also, when algae are nutrient deprived (e.g., to trigger lipid production (Hu et al. 2008)), the value of the half-saturation constant will play a more important role in algae growth.

To properly model the effect of nutrients, we must ensure appropriate amounts of nutrients are removed from the simulation with increased algae concentration. Algae atomic composition ratio was measured at the end of the greenhouse experiment on day 7 yielding a C/N/P ratio of 358:38:1. For reference, the Redfield ratio for marine plankton in open oceans is 106:16:1 (Redfield 1934). Significant variability of elemental composition exists across strains and even within strains due to environmental stressors and adaptations. Nutrients recycle in the system as algae metabolize the inorganic forms of nitrate and phosphate into their dissolved organic forms. These dissolved organic nitrates and phosphates are mineralized back into their inorganic forms at rates of 0.015 and 0.1 day⁻¹ (Cercu and Cole 1995). All

of these water quality variables are tracked in the model.

Light

The growth of algae is a strong function of irradiance, which is a function of average daylight, light extinction, light intensity at the water surface, optimal light intensity, and depth of the algae below the water surface. Algae grow as the light intensity increases to some saturation (optimum) intensity (I_s), beyond which growth rates decline due to photo inhibition. The function for non-optimal illumination is derived from Steele’s equation (DiToro et al. 1971; DiToro and O’Connor 1975):

$$g(I) = \frac{I(z)}{I_s} e^{1 - \frac{I(z)}{I_s}} \tag{7}$$

where $I(z)$ is the instantaneous light intensity at depth z and I_s is the optimal light intensity. If the growth medium is not well-mixed, then the rate of change of light intensity $I(z)$ changes with depth (or model layer) due to non-uniform growth of algae. If, on the other hand, the system is well-mixed, then the biomass concentration will be homogeneous (constant light extinction). For such a system (i.e., the single-layer model studied in this work), the growth limitation is:

$$g(I) = \frac{e}{K_c d} (e^{-\alpha_1} - e^{-\alpha_0}) \tag{8}$$

where d is the water-layer depth, K_c is the light extinction coefficient, α_0 is the light intensity ratio at the top of the water surface:

$$\alpha_0 = \frac{I_0}{I_s} \tag{9}$$

and α_1 , the ratio at the bottom (of the layer), is:

$$\alpha_1 = \frac{I_0}{I_s} e^{-K_c d} \tag{10}$$

Note that recursive calculations are necessary for multilayer models.

The light extinction coefficient, K_c , in a single-layer model and within a particular layer in a multilayer hydrodynamics model is considered to be a constant and formulated as

$$K_c = k_b + k_c B \tag{11}$$

where k_b is the constant background light extinction coefficient due to water and other suspended particulates and k_c is

the constant light extinction due to suspended carbon (or biomass) concentration in the layer. A standard value of 0.1 m^{-1} is used for k_b (Cercu and Cole 1995).

The absorptivity curve that yields the light extinction coefficient, k_c , was generated for *N. salina* grown in the laboratory. Because the majority of light is absorbed by the chlorophyll and the light absorbed by chlorophyll contributes greatest to the growth, the light extinction coefficient was calculated for the wavelength of peak chlorophyll absorption. At 678 nm, the light extinction value was calculated to be $0.3501 \text{ m}^2 \text{ g}^{-1} \text{ C}$. The concentration-dependent absorptivity is calculated from measured values in terms of cell count ($4.19 \times 10^{-9} \text{ mL cell}^{-1} \text{ cm}^{-1}$), the measured cell mass of 2.7 pg cell^{-1} , which is similar to reported values for *Nannochloropsis* (Briassoulis et al. 2010), and the estimated fraction of carbon in biomass as $0.45 \text{ g C g}^{-1} \text{ B}$.

The optimal light intensity was fit to the lab-scale growth rate data to determine $I_s = 20 \text{ W m}^{-2}$. Although the growth rate continued to increase slightly at higher light levels, the health of the algae appeared to deteriorate in the higher light conditions as the algae pigment changed from green to yellow.

Temperature

Algal growth rate increases with temperature up to an optimal and decreases at temperatures beyond the optimal (Cossins and Bowler 1987). Temperature effects are defined by an exponential function of water temperature, the optimal temperature for growth, and the temperature effect coefficients below and above the optimal temperatures:

$$h(T) = \begin{cases} \exp[-K_1^T(T-T_1)^2] & \text{for } T \leq T_1 \\ 1 & \text{for } T_1 < T \leq T_2 \\ \exp[-K_2^T(T_2-T)^2] & \text{for } T > T_2 \end{cases} \quad (12)$$

where T is the local temperature from the hydrodynamic model, T_1 is the lower optimal growth temperature, T_2 is the upper optimal growth temperature, K_1^T is the temperature effect below the optimal growth temperature, and K_2^T is the temperature effect above the optimal growth temperature.

The fitted lower and upper optimal growth temperatures are 21.5 and 23.5 °C, respectively. These values are lower than the 26–28 °C values reported by others for this strain, but are consistent with other measurements made on our lab's version of the strain (James et al. 2013; Huesemann et al. 2013; Boussiba et al. 1987). The fitted temperature effects below and above optimal are 0.015 and 0.01 °C⁻², respectively. The resulting R^2 for the temperature parameter fitting was 0.8.

Salinity

Marine algae growth rates have an optimum salinity above and below which the growth rate decreases (Brock 1975; Auken and McNulty 1973; García et al. 2007; Fabregas et al. 1984; Batterton and Baalen 1971). The salinity of the media is limited to a range between zero for a completely non-saline solution to its maximum solubility in water. The effect of salinity on algae growth has yet to be formulated into a general equation that can be applied to a variety of halotolerant/halophilic algae species. Given the similarity in curve shape to temperature, we propose an exponential function for salinity:

$$i(S) = \begin{cases} \exp[-k_{s_1}(S-S_{\text{opt}})^2] & \text{for } S \leq S_{\text{opt}} \\ \exp[-k_{s_2}(S-S_{\text{opt}})^2] & \text{for } S > S_{\text{opt}} \end{cases} \quad (13)$$

where S is the salinity, S_{opt} is the optimal salinity, k_{s_1} is the salinity effect below the optimal salinity, and k_{s_2} is the salinity effect above the optimal salinity.

The fitted optimal NaCl concentration is 20 ppt or 0.35 M and the fitted salinity effect above optimal is $9 \times 10^{-4} \text{ ppt}^{-2}$, salinities below the optimal value were not studied so the sub-optimal-effect parameter is assumed equal to the super-optimal. The resulting R^2 for the salinity parameter fitting was 0.9. The optimal salinity measured is less than that previously measured for a similar strain, but given the long period that our strain was grown in *f/2* and the other differences between strains, this is not unexpected (Boussiba et al. 1987).

To determine the parameters for the growth model described above, lab-scale experiments were conducted and the parameters were fit to the data. In the following section, we describe how we verified the parameter fitting by simulating the lab-scale experiments and ensuring that we predict the growth appropriately. Subsequently, we validated the model scale-up by comparing it to both the modeled and the experimental results of larger scale systems.

Results and discussion

Lab scale

The developed empirical fits were supplied to the model and compared with the lab-scale measurements and ensure that the model is appropriately parameterized. The model was set up in the simplified well-mixed domain with dimensions of $15 \times 2.2 \times 2.2 \text{ cm}^3$ for the representative rectangular culture volume of the test tubes used in the experiments (equivalent volume and depth). The modeled test tube is exposed to light from one side at the specified intensities. The initial nutrient

concentrations for the $f/2$ medium were 2.3 mM NO_3 (32.2 g m^{-3}) and 0.067 mM PO_4 (2.075 g m^{-3}). The initial CO_2 concentration was 0.9 g m^{-3} (Burkhardt et al. 1999). The absorption of CO_2 into the media from the bubbling of air is assumed to be sufficient to sustain this amount of CO_2 ($2.31 \mu\text{g s}^{-1}$). The initial algae concentrations were set to the initial measured concentrations.

The resulting parameters for the ideal growth conductions for *N. salina* are a NaCl concentration of $S_{\text{opt}}=0.35 \text{ M NaCl}$, a light intensity of $I_s=20 \text{ W m}^{-2}$, and temperatures between $T_1=21.5$ and $T_2=23.5 \text{ }^\circ\text{C}$. The theoretical maximum growth rate at ideal conditions, P_M , from Eq. (2) was used to fit the model to the measurements and was determined to be 2.5 day^{-1} . Using this value, the model generally replicates the data well. The resulting R^2 value is 0.79. Figure 2 shows the algae concentrations from measurements and simulations over time at temperatures of 18, 22, 26, and $30 \text{ }^\circ\text{C}$, respectively, for various light intensities and NaCl concentrations.

The maximum measured daily average growth rate in the lab-scale study was 0.55 day^{-1} , which when divided by $2/3$ for the fraction of the day with light gives $\overline{P-B_M} = 0.825 \text{ day}^{-1}$ the maximum average daily growth rate observed, which includes reductions due to non-ideal conditions and basal metabolism. The expected trends were observed; growth rates decreased at temperatures and salinities above and below the optimal values. Growth rates also diminished at light intensities below the optimal intensity and leveled out at higher intensities. Although pigment change was observed at the highest light intensity (green to yellow), no decrease in growth rate was observed. The maximum instantaneous growth rate found in the simulation was $P-\delta B_M=1.3 \text{ day}^{-1}$, which includes reductions due to non-ideal conditions and uncertainty in basal metabolism, δB_M .

Greenhouse tanks

To validate the model and show its potential to predict larger scale systems, it must be compared with a larger scale

measurement that is completely independent of the growth rate function parameterization. As a first step in validation of the model and its scalability, the parameter values obtained from the laboratory measurements are applied to the greenhouse setup. Two tanks are simulated as fully mixed $1.67 \times 1.5 \text{ m}^2$ rectangular tanks with a 0.211-m depth consisting of approximately 0.53 m^3 of medium. The light and water temperature measured in the tank cultures over the course of the 7-day experiment are shown in Fig. 3. The CO_2 absorbed into the medium from the bubbling is calculated using the same method as James et al. (2013).

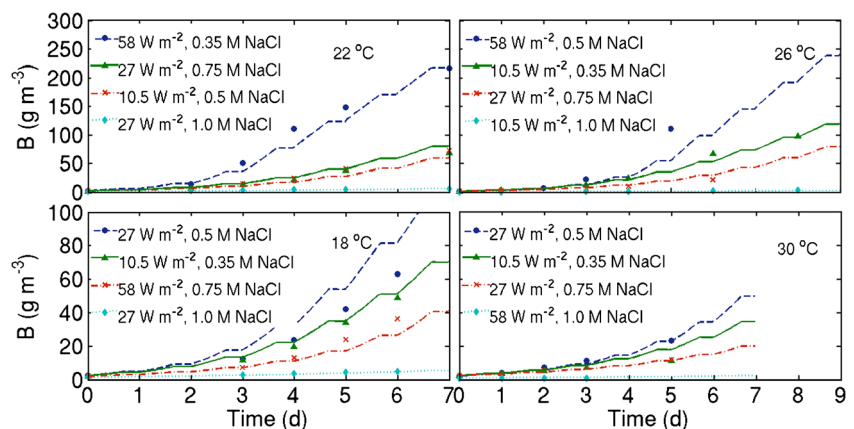
The results from the measurements and the model are plotted in Fig. 4. The model reasonably predicts the algae concentration for each tank operating with different CO_2 sources. The resulting R^2 values were 0.91 for the tank bubbled at $85 \text{ L h}^{-1} \text{ CO}_2$ and 0.83 for the tank bubbled with air only.

The three most significant parameters limiting algal growth are light, temperature, and CO_2 concentration. The limitation factors for each of these are plotted in Fig. 5. For this case, the ideal light and temperature are well aligned due to diurnal fluctuations. However, the CO_2 concentration becomes limiting during high-growth periods under ideal light and temperature conditions, both of which limited growth even during high- CO_2 concentration bubbling. The maximum simulated instantaneous growth rate for the conditions of the experiment was $P-\delta B_M=1.2 \text{ day}^{-1}$.

Open-channel raceway

Given that the model with the simplified domain reasonably simulated the greenhouse tanks, it was extended to an open-channel raceway system. The optimal parameter values from the laboratory experiment (I_s , S_{opt} , T_1 , and T_2) were again applied to the experimental open-channel raceway. The raceway was simulated as well-mixed with simplified domain $24.3 \times 2.44 \text{ m}^2$ rectangular pond with a 0.20-m depth and 11.9 m^3 of medium. Sufficient CO_2 is assumed because the growth in the pond is greatly limited by the temperature, pH

Fig. 2 Plot of the predicted (curves) and measured (symbols) algae concentration over time comparison at 18, 22, 26, and $30 \text{ }^\circ\text{C}$ for various representative light intensity and salinity conditions at the lab scale



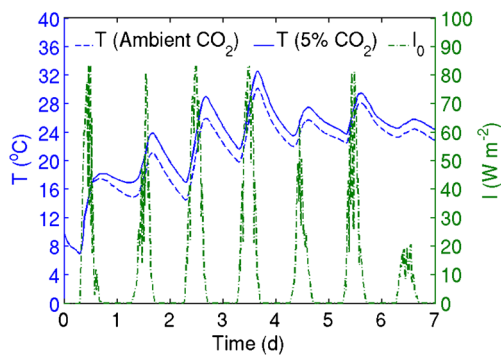


Fig. 3 Plot of the measured temperature for the 5 % CO₂ (solid) and ambient CO₂ (dashed) and light intensity (dash-dot) experienced by the greenhouse tanks over the course of the measurement

remained relatively constant, and CO₂ is introduced to the culture through an air stone sparger and paddle wheel mixing.

The model greatly under predicts the algae growth for this case. The resulting R^2 value for this case is only 0.63, which suggests that at least one of the model assumptions was not valid. The question is: to what degree are differences in algae strains, scale up, and the fully mixed assumption the source of disagreement? The two largest contributors to limiting algal growth for this case are light and water temperature with measured data shown in Fig. 6. The limitation factors for each of these are plotted in Fig. 7. For this case, the ideal light and temperature are not well aligned. When the light is sufficient, the temperature of the pond is above its optimal value. When the light is limiting, the temperature reduces to more optimal values. This causes most of the growth to occur in the morning and evening periods, while at mid-day and at night the growth is limited and zero, respectively.

Recent research has shown that the mixing in these large raceway ponds is much less than in the laboratory test tubes or the jet mixed greenhouse tanks (Mendoza et al. 2013; Singh et al. 2012; Bernard et al. 2013). Mendoza et al. (2013) found mixing times ranging between 1.4 and 6 h (nearly half of the daylight). Singh et al. (2012) found that the vertical mixing rates were only 0.5 % of the longitudinal mixing times.

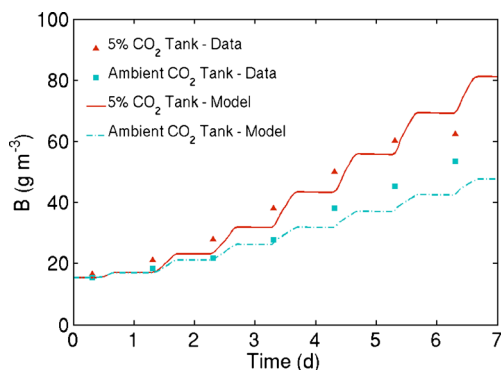


Fig. 4 Plot of the measured (symbols) and modeled (curves) algae concentrations over time for the greenhouse tanks at 5 % (solid/triangle) and ambient (dash-dot/square) CO₂ bubbling concentrations

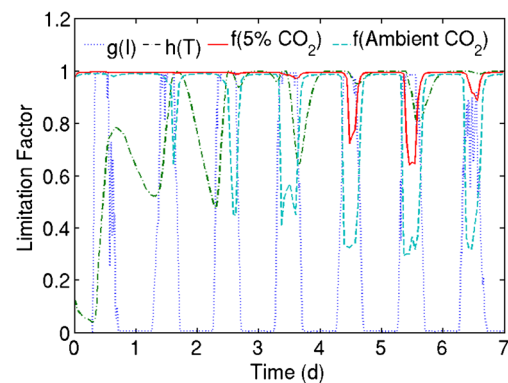


Fig. 5 Plot of the limitation factors over time for the greenhouse ponds for light (dotted), temperature (dash-dot), and CO₂ at 5 % (solid) and ambient (dashed) bubbling concentrations

Bernard et al. (2013) showed that except for at the paddle wheel, very little vertical mixing occurs. The algae concentrations were much higher in the raceway than in either the lab or the greenhouse ponds. The resulting self-shading becomes more important, while the reduced mixing causes a non-uniform algae concentration. This nonlinear effect cannot be appropriately accounted for by a simple well-mixed model. The light intensity and environmental effects, however, were much higher for the raceway measurement than either the lab or greenhouse, which may result in large temperature variations with depth. Given the high concentration of algae and high variability of light and temperature with depth, the algae concentration will also vary with depth and the fully mixed assumption is not appropriate for this system.

To relax the fully mixed assumption, the temperature variation with depth is calculated. This requires heat transfer calculations within the pond and between the pond and its surroundings including the effects produced by convection with the air, evaporation, conduction through the bottom of the raceway, and radiation to the atmosphere and from the sun.

The temperature is calculated by performing an energy balance at the surface of the pond. Given the small penetration depth of infrared light in water compared to the depth of the

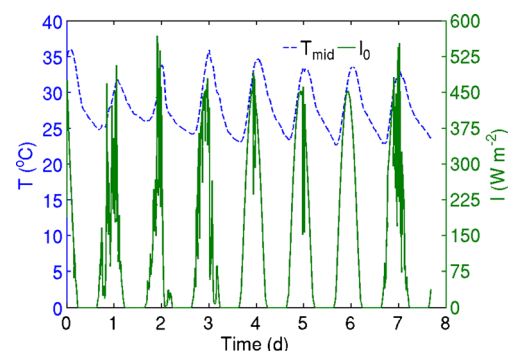


Fig. 6 Plot of the measured temperature (dashed) and light intensity (solid) experienced by the open-channel raceway over the course of the measurement

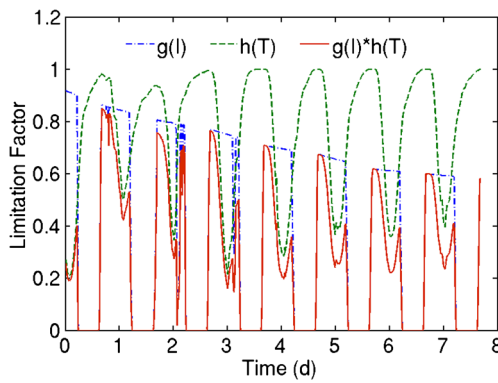


Fig. 7 Plot of the limitation factors for light (*dash-dot*), temperature (*dashed*), and their combined limitation (*solid*) over time for the open-channel raceway

pond (majority of IR radiation is absorbed in the first 1-2 cm (Hale and Querry 1973; Kou et al. 1993)), the heat flux from radiation can simply be applied to the surface. Two types of radiation must be accounted for, the shortwave radiation, which is essentially the measured solar radiation obtained from a weather station, and the longwave radiation, which is typically not detected by the sensors and must be calculated. The heat flux due to longwave radiation, q''_{lw} , is given by:

$$q''_{lw} = \varepsilon_s \sigma (T_{sky}^4 - T_s^4) \tag{14}$$

where σ is the Stefan Boltzmann constant, ε_s is the emissivity of water, T_s is the temperature of the water surface, and T_{sky} is the temperature of the sky, which can be estimated from experimental data or empirical relationships (Martin and Berdahl 1984).

Heat flux due to convection, q''_{conv} , between the pond surface and the surrounding air is given by:

$$q''_{conv} = \bar{h}(T_\infty - T_s) \tag{15}$$

where \bar{h} is the average convective heat transfer coefficient, and T_∞ is the temperature of the surrounding air. The average

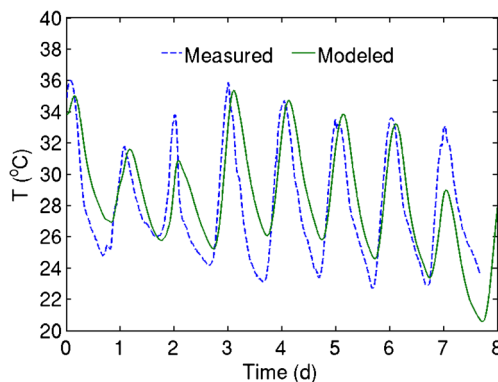


Fig. 8 Plot of the measured (*dashed*) and modeled (*solid*) temperatures 10 cm below the water surface

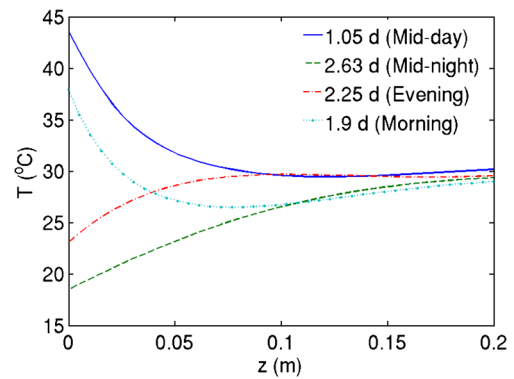


Fig. 9 Plot of the modeled temperatures versus depth at representative times during the day: mid-day (*solid*), mid-night (*dashed*), evening/dusk (*dash-dot*), and morning/dawn (*dotted*)

convective heat transfer coefficient depends on the system geometry and the turbulent nature of the air flow (Incropera 2007). For laminar flow, it is given by:

$$\bar{h} = \frac{k_a}{L} (0.644 Re_L^{1/2} Pr^{1/3}) \tag{16}$$

where k_a is the thermal conductivity of the air, L is the length of the pond surface, Re is the Reynolds number, and Pr is the Prandtl number. For turbulent flow, it is given by:

$$\bar{h} = \frac{k_a}{L} (0.037 Re_L^{4/5} - 871) Pr^{1/3} \tag{17}$$

Heat flux due to evaporation, q''_{evap} , depends on the latent heat of vaporization, h_{fg} , and the amount of water being evaporated and is given by:

$$q''_{evap} = h_{fg} h_m (c_{sat} - c_\infty) \tag{18}$$

where h_m is the mass transfer coefficient, c_{sat} is the saturation value for the water vapor concentration, and c_∞ is the value of the water vapor concentration in the surrounding air. The mass transfer coefficient is related to the

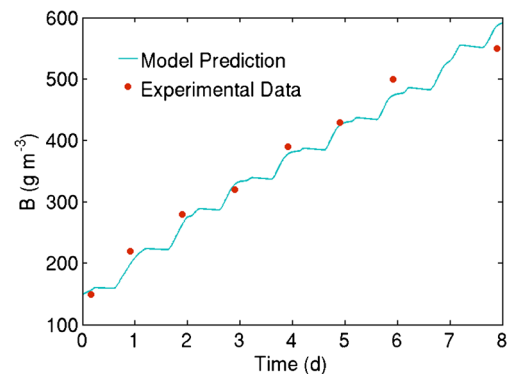


Fig. 10 Plot of the measured (*circle*) and predicted (*solid curve*) algae concentrations over time for the open-channel raceway accounting for variation of light and temperature with depth

convective heat transfer coefficient by the heat and mass transfer analogy:

$$\frac{h}{h_m} = \rho C_p Le^{1-n} \quad (19)$$

where ρ is the air density, C_p is the air specific heat, Le is the Lewis number, and n is a constant approximated as 1/3 (Incropera 2007).

Finally, the conductive heat flux, q''_{cond} , occurs between the ground and pond and is given by:

$$q''_{\text{cond}} = \frac{k_g}{L_g}(T_{\text{bot}} - T_g) \quad (20)$$

where T_{bot} is the temperature of the bottom of the pond, T_g is the temperature of ground, L_g is the distance into the ground the measurement is made, and k_g is the thermal conductivity of the ground, which can be determined based on experimental data and will depend on soil type and moisture content. These heat fluxes are then applied to the model as boundary conditions on the appropriate surfaces to determine the spatiotemporal variation of temperature within the pond.

Weather data for Mesa, Arizona, was acquired from the Arizona Meteorological Network and included air and ground temperatures, solar radiation, relative humidity, and wind speed. Figure 8 is a comparison between the predicted and measured temperature during cultivation 10 cm from the water surface. The model reasonably matches the measured temperature values. On day 7, flocculation was observed on the surface of the pond, which affected the pond temperature and caused a deviation between the measured and predicted temperatures.

The temperature calculation allows us to estimate the temperature as a function of depth with the assumption of non-ideal pond mixing. Figure 9 shows the predicted temperature variation with depth at different representative times of the day. At mid-day, for instance, the solar radiation and air temperature are relatively high in an outdoor pond and the radiation and convection occur at the surface; consequently, the surface temperature of the water rises much faster than the deeper water of the raceway. Likewise, in the evening, heat escapes from the surface causing the temperature of the water near the surface to decrease more rapidly. The temperature variation on the surface closely resembles that measured by (Reichardt et al. 2013) at a similar raceway with a spectroradiometer that also gives an in situ measurement of biomass and pigment optical activity. Consequently, because the light intensity is attenuated with depth, the interplay between the light and temperature over the course of the day is important for estimating algae growth.

Accounting for variations in light and temperature with depth yields a much better agreement between the model and the measurements. Figure 10 compares modeled and measured values. The resulting R^2 value is 0.97.

Conclusions

Multifactorial measurements of *N. salina* were conducted to populate the empiricisms for an algae growth kinetics model. The effect of salinity on growth was added to the base CEQUAL model to simulate marine algal species. The laboratory-parameterized model for *N. salina* was scaled up to simulate two larger, outdoor experimental studies. The model accurately predicted the growth trends in greenhouse tanks using a simplified well-mixed domain and an open-channel raceway using a more complex domain accounting for spatial variations in temperature and light intensity. The model (using parameters derived from the lab-scale experiment) was used to determine which environmental factors are most limiting to growth (light and temperature). This model could also be used to study the scale-up effect through comparisons of the lab-scale kinetics and a larger scale system including the effects of predation, depth-decay of light (light extinction), and optimized nutrient and CO₂ delivery. The model could be expanded to study growth in production-scale photobioreactors and open-channel raceways, thus eliminating the need for expensive large-scale experiments. As more multifactorial data are accumulated for a variety of algal strains, the model could be used to select appropriate algal species for various geographic and climatic locations.

Acknowledgments The authors would like to thank Dr. Todd Lane and Pam Lane from Sandia National Laboratories for their guidance with the lab-scale algae growth and measurement methods, Brian Dwyer from Sandia National Laboratories for maintaining the greenhouse, Kathleen Alam from Sandia National Laboratories for providing access to her laboratory equipment enabling the absorptivity measurements, Dave van Nom at the University of New Mexico for lending data logging instrumentation for the greenhouse experiments, and the University of New Mexico Biology Analytical Annex for providing the C/N/P analysis of the media and biomass. This work was supported by the Laboratory Directed Research and Development program at Sandia National Laboratories. Sandia National Laboratories is a multi-program laboratory managed and operated by Sandia Corporation, a wholly owned subsidiary of Lockheed Martin Corporation, for the US Department of Energy's National Nuclear Security Administration under contract DE-AC04-94AL85000.

References

- Auken OWV, McNulty IB (1973) The effect of environmental factors on the growth of a halophilic species of algae. *Biol Bull* 145:210–222
- Bartley ML, Boeing WJ, Dungan BN, Holguin FO, Schaub T (2013) pH effects on growth and lipid accumulation of the biofuel microalgae *Nannochloropsis salina* and invading organisms. *J Appl Phycol*. doi:10.1007/s10811-013-0177-2
- Batterton JC, Baalen CV (1971) Growth response of blue-green algae to sodium chloride concentration. *Arch Microbiol* 76:151–165
- Bernard O, Boulanger A-C, Bristeau M-O, Sainte-Marie J (2013) A 2D model for hydrodynamics and biology coupling applied to algae growth simulations. *Esaim-Math Model Num* 47:1387–1412

- Boussiba S, Vonshak A, Cohen Z, Avissar Y, Richmond A (1987) Lipid and biomass production by the halotolerant microalga *Nannochloropsis salina*. *Biomass* 12:37–47
- Briassoulis D, Panagakos P, Chionidis M, Tzenos D, Lalos A, Tsinos C, Berberidis K, Jacobsen A (2010) An experimental helical-tubular photobioreactor for continuous production of *Nannochloropsis* sp. *Bioresour Technol* 101:6768–6777
- Brock TD (1975) Salinity and the ecology of *Dunaliella* from Great Salt Lake. *J Gen Microbiol* 89:285–292
- Burkhardt S, Zondervan I, Riebesell U (1999) Effect of CO₂ concentration on C:N:P ratio in marine phytoplankton: a species comparison. *Limnol Oceanogr* 44:683–690
- Cerco CF, Cole T (1994) Three-dimensional eutrophication model of Chesapeake Bay. US Army Corps of Engineers
- Cerco CF, Cole T (1995) User's guide to the CE-QUAL-ICM three-dimensional eutrophication model, Release Version 1.0. U.S. Army Corps of Engineers
- Chisti Y (2007) Biodiesel from microalgae. *Biotechnol Adv* 25:294–306
- Cossins AR, Bowler K (1987) Temperature biology of animals. Chapman and Hall, New York
- DiToro DM, O'Connor DJ (1975) Phytoplankton–zooplankton–nutrient interaction model for Western Lake Erie. *Ecology* 3:423–473
- DiToro D, O'Connor S, Thomann R (1971) A dynamic model of the phytoplankton population in the Sacramento-San Joaquin Delta. In: Nonequilibrium systems in water chemistry. American Chemical Society, Houston, pp 131–180
- Eppley RW (1972) Temperature and phytoplankton growth in the sea. *Fish Bull* 70:1063–1085
- Fabregas J, Abalde J, Herrero C, Cabezas BV, Veiga M (1984) Growth of the marine microalga *Tetraselmis suecica* in batch cultures with different salinities and nutrient concentrations. *Aquaculture* 42:207–215
- Fluent (2012) Fluent user's guide. 13.1 edn. ANSYS, Inc
- García F, Freile-Pelegrián Y, Robledo D (2007) Physiological characterization of *Dunaliella* sp. (Chlorophyta, Volvocales) from Yucatan, Mexico. *Bioresour Technol* 98:1359–1365
- Guillard RRL, Ryther JH (1962) Studies of marine diatoms. I. *Cyclotella nana* Husdelt and *Detonula confervacea* (Cleve) Gran. *Can J Microbiol* 8:229–239
- Haaland DM, Easterling RG, Vopicka DA (1985) Multivariate least-squares methods applied to the quantitative spectral analysis of multicomponent samples. *Appl Spectrosc* 39:73–84
- Hale GM, Query MR (1973) Optical constants of water in the 200-nm to 200- μ m wavelength region. *Appl Optics* 12:555–563
- Hecky RE, Campbell P, Hendzel LL (1993) The stoichiometry of carbon, nitrogen, and phosphorus in particulate matter of lakes and oceans. *Limnol Oceanogr* 38:709–724
- Hu Q, Sommerfeld M, Jarvis E, Ghirardi M, Posewitz M, Seibert M, Darzins A (2008) Microalgal triacylglycerols as feedstocks for biofuel production: perspectives and advances. *Plant J* 54:621–639
- Huesemann MH, Wagenen JV, Miller T, Chavis A, Hobbs S, Crowe B (2013) A screening model to predict microalgae biomass growth in photobioreactors and raceway ponds. *Biotechnol Bioeng* 110:1583–1594
- Incropera FP (2007) Fundamentals of heat and mass transfer, 6th edn. John Wiley, Hoboken
- James SC, Boriah V (2010) Modeling algae growth in an open-channel raceway. *J Comput Biol* 17:895–906
- James SC, Janardhanam V, Hanson DT (2013) Simulating pH effects in an algal-growth hydrodynamics model. *J Phycol* 49:608–615
- Katz A, Bental M, Degani H, Avron M (1991) In vivo pH regulation by a Na⁺/H⁺ antiporter in the halotolerant alga *Dunaliella salina*. *Plant Physiol* 96:110–115
- Kirst GO (1989) Salinity tolerance of eukaryotic marine algae. *Annu Rev Plant Physiol* 40:21–53
- Kou L, Labrie D, Chylek P (1993) Refractive indices of water and ice in the 0.65- to 2.5 μ m spectral range. *Appl Optics* 32:3531–3540
- Laurens LML, Dempster TA, Jones HDT, Wolfrum EJ, Wychen S, McAllister JSP, Rencenberger M, Parchert KJ, Gloe LM (2012) Algal biomass constituent analysis: method uncertainties and investigation of the underlying measuring chemistries. *Anal Chem* 84:1879–1887
- Lewis LA, Lewis PO (2005) Unearthing the molecular phylodiversity of desert soil green algae (Chlorophyta). *Syst Biol* 54:936–947
- Li Z, Wakao S, Fischer BB, Niyogi KK (2009) Sensing and responding to excess light. *Annu Rev Plant Biol* 60:239–260
- Liffman K, Paterson DA, Liovic P, Bandopadhyay P (2013) Comparing the energy efficiency of different high rate algal raceway pond designs using computational fluid dynamics. *Chem Eng Res Design* 91:221.226
- Martin M, Berdahl P (1984) characteristics of infrared sky radiation in the United States. *Sol Energy* 33:321–336
- Masojidek J, Vonshak A, Torzillo G (2010) Chlorophyll fluorescence applications in microalgal mass cultures. In: Suggett DJ, Prasil O, Borowizka MA (eds) Chlorophyll *a* fluorescence in aquatic sciences: methods and applications. Springer, Dordrecht, pp 277–292
- Mata TM, Martins AA, Caetano NS (2010) Microalgae for biodiesel production and other applications: a review. *Renew Sust Energ Rev* 14:217–232
- MATLAB (2013) MATLAB primer. R2013a edn. MathWorks, Inc
- Mayer P, Cuhel R, Nyholm N (1997) A simple in vitro fluorescence method for biomass measurements in algal growth inhibition tests. *Water Res* 31:2525–2531
- Mayo AW (1997) Effects of temperature and pH on the kinetic growth of unialga *Chlorella vulgaris* cultures containing bacteria. *Water Environ Res* 69:64–72
- Mendoza JL, Granados MR, Godos I, Acien FG, Molina E, Banks C, Heaven S (2013) Fluid-dynamic characterization of real-scale raceway reactors for microalgae production. *Biomass Bioenergy* 54:267–275
- Monod J (1949) The growth of bacterial cultures. *Annu Rev Microbiol* 3:371–394
- Pal D, Khozin-Goldberg I, Cohen Z, Boussiba S (2011) The effect of light, salinity, and nitrogen availability on lipid production by *Nannochloropsis* sp. *Appl Micro Cell Physiol* 90:1429–1441
- Quinn J, Winter L, Bradley T (2011) Microalgae bulk growth model with application to industrial scale systems. *Bioresour Technol* 102:5083–5092
- Redfield AC (1934) On the proportions of organic derivatives in sea water and their relation to the composition of plankton. In: Daniel RJ (ed) James Johnstone memorial volume. University Press of Liverpool, London, pp 176–192
- Reichardt TA, Collins AM, Timlin JA, McBride RC, Behnke CA (2013) Spectroradiometric monitoring of open algal cultures. Conference on lasers and electro-optics. The Optical Society, San Jose
- Remias D, Lütz-Meindl U, Lütz C (2005) Photosynthesis, pigments and ultrastructure of the alpine snow alga *Chlamydomonas nivalis*. *Eur J Phycol* 40:259–268
- Samuelsson G, Öquist G (2006) A method for studying photosynthetic capacities of unicellular algae based on in vivo chlorophyll fluorescence. *Physiol Plant* 40:315–319
- Serôdio J, Marquês da Silva J, Catarino F (2001) Use of in vivo chlorophyll *a* fluorescence to quantify short-term variations in the productive biomass of intertidal microphytobenthos. *Mar Ecol Prog Ser* 218:45–61
- Singh J, Gu S (2010) Commercialization potential of microalgae for biofuels production. *Renew Sust Energ Rev* 14:2596–2610
- Singh S, Ahmad Z, Kothiyari UC (2012) Mixing coefficients for longitudinal and vertical mixing in the near field of a surface pollutant discharge. *J Hydraul Res* 48:91–99

- Sukenik A, Beardall J, Kromkamp JC, Kopecky J, Masojidek J, Bergeijk S, Gabai S, Shaham E, Yamshon A (2009) Photosynthetic performance of outdoor *Nannochloropsis* mass cultures under a wide range of environmental conditions. *Aquat Microb Ecol* 56:297–308
- Sun A, Davis R, Starbuck M, Ben-Amotz A, Pate R, Pienkos PE (2011) Comparative cost analysis of algal oil production for biofuels. *Energy* 36:5169–5179
- Torzillo G, Accolla P, Pinzani E, Masojidek J (1996) In situ monitoring of chlorophyll fluorescence to assess the synergistic effect of low temperature and high irradiance stresses in *Spirulina* cultures grown outdoors in photobioreactors. *J Appl Phycol* 8:283–291
- US-DOE (2009) National algal biofuels technology roadmap. Office of Energy Efficiency and Renewable Energy and Office of Biomass, Albuquerque
- Vyhnalek V, Fisar Z, Fisarova A, Komarkova J (1993) In vivo fluorescence of chlorophyll *a*: estimation of phytoplankton biomass and activity in Rimov Reservoir (Czech Republic). *Water Sci Technol* 28:29–33